

# Green Chemistry

Accepted Manuscript



This is an *Accepted Manuscript*, which has been through the Royal Society of Chemistry peer review process and has been accepted for publication.

*Accepted Manuscripts* are published online shortly after acceptance, before technical editing, formatting and proof reading. Using this free service, authors can make their results available to the community, in citable form, before we publish the edited article. We will replace this *Accepted Manuscript* with the edited and formatted *Advance Article* as soon as it is available.

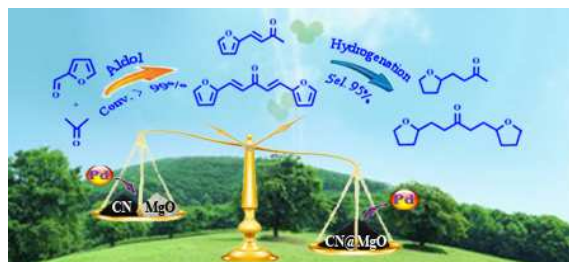
You can find more information about *Accepted Manuscripts* in the [Information for Authors](#).

Please note that technical editing may introduce minor changes to the text and/or graphics, which may alter content. The journal's standard [Terms & Conditions](#) and the [Ethical guidelines](#) still apply. In no event shall the Royal Society of Chemistry be held responsible for any errors or omissions in this *Accepted Manuscript* or any consequences arising from the use of any information it contains.



[www.rsc.org/greenchem](http://www.rsc.org/greenchem)

## Table of Contents



A bifunctional catalyst Pd/CN@MgO showed excellent catalytic activity in the above tandem reaction, achieving full conversion and nice products selectivity.

Cite this: DOI: 10.1039/c0xx00000x

www.rsc.org/xxxxxx

ARTICLE TYPE

# Ultrafinely Dispersed Pd Nanoparticles on a CN@MgO Hybrid as a Bifunctional Catalyst for Bioderived Compounds Upgrading

Mingming Li, XuanXu, Yutong Gong, Zhongzhe Wei, Zhaoyin Hou, Haoran Li and Yong Wang\*

Received (in XXX, XXX) XthXXXXXXXXXX 20XX, Accepted Xth XXXXXXXXXXXX 20XX

DOI: 10.1039/b000000x

A novel and sustainable synthesis of Pd/CN@MgO catalyst is presented here, offering a bifunctional catalyst with high catalytic activity towards a tandem aldol condensation-hydrogenation reaction of furfural with acetone in a one-pot reactor. The incorporation of biomass based hydrophilic N-containing carbon (CN) in the catalyst provides a subtle but elegant method to control the good dispersion in water, the reaction stability, and ultrafinely dispersed palladium particles (2.2 nm in average size) of the bifunctional catalyst Pd/CN@MgO. With such improved features, an impressive 99% furfural conversion and 95% hydrogenation products (saturated ketones) selectivity was obtained by using Pd/CN@MgO as a novel bifunctional catalyst in the present tandem reaction. This catalyst designing strategy and the high efficiency of the catalyst in the catalytic system offer potentials for bi/multifunctional catalysts preparation and one-pot synthesis of bioderived intermediates.

## Introduction

Heterogeneous catalysts, with their advantage of being easily separated from the reactants and products of the overall catalytic process, have been an appealing research topic in recent years.<sup>1</sup> As the selection of heterogeneous catalysts offers special challenges, much effort has been focused on the design and synthesis of new efficient, simple, and sustainable materials as catalysts or catalyst supports.

Among the various heterogeneous catalysts, supported catalysts are frequently used. In particular, catalyst supports play significant roles in reaction performance. Among the various supports, metal oxides (e.g. Al<sub>2</sub>O<sub>3</sub>, MgO, ZrO<sub>2</sub>, CeO<sub>2</sub> and SiO<sub>2</sub>),<sup>2-5</sup> zeolites,<sup>6</sup> metal-organic framework (MOF)<sup>7, 8</sup> and carbons (including carbon black, activated carbon, graphene, carbon nanofiber, carbon nanotube, and carbon sphere)<sup>9-14</sup> are frequently used. However, these catalyst supports may suffer from problems like ununiform particle size with poor dispersion, weak particle-support bonding, poor water dispersion, or reaction monofunctionality. Intriguingly, recent years have witnessed increased interests in developing hybrids as catalyst supports with enhanced catalytic performance.<sup>15-18</sup> Notably, bifunctional or multifunctional catalysts, with their advantage of simplifying reaction processes without dealing with some separation or treatment procedures caused by individual operation,<sup>19</sup> have recently attracted intensive studies.<sup>18, 20,21</sup> Therefore, developing a novel bifunctional catalyst with enhanced catalytic activity is desirable.

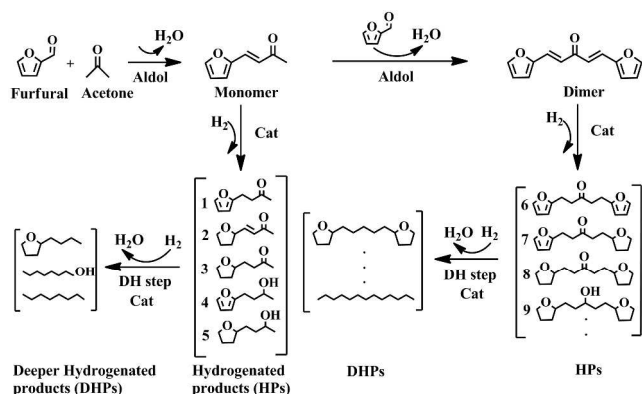
Biomass, as a green, sustainable and cheap resource easily available in the wild, can be directly made into various kinds of carbon materials.<sup>22-24</sup> Recently, an intriguing method of incorporating nitrogen into the structure of carbon materials has

gained increasing interest, as some beneficial effects on the physicochemical properties like electrical conductivity, basicity, and catalytic activity with obvious modifications and enhancements have been demonstrated.<sup>25-27</sup> Still, the doped nitrogen heteroatom on carbon supports has shown the ability to stabilize noble metal (e.g. Pd, Pt) NPs due to the activation of neighboring carbon atoms by the electron affinity of nitrogen,<sup>28,29</sup> which is rather beneficial for heterogeneous catalysts.<sup>30</sup> Recently, much of our work has also been on developing N-containing carbon supported catalysts, and satisfying results were obtained.<sup>10, 14,31-33</sup> However, due to their relatively neutral property, these N-containing carbon supported catalysts are only restricted to monofunctionality. Heterogeneous basic MgO catalyst, with its ability in triggering certain reactions like condensation reactions,<sup>18, 34</sup> has been widely studied, but it encounters problems like inferior hydrothermal stability and water dispersions to carbon materials. Attractively, if they are hybridized in an appropriate manner, we may envision that a bifunctional catalyst with enhanced properties can be formed while retaining their advantages but discharging their deficiencies.

Recent years have witnessed an increasing interest in developing renewable energy resources as alternatives to the diminishing non-renewable fossil fuels. Carbohydrates constitute the largest fraction of biomass feedstock, and they can be converted into various platform molecules from which tailor-made products can be achieved through specific catalytic steps. Among the various intermediates are 5-hydroxymethylfurfural (HMF) and furfural (FF), which are accessible from saccharides (a common component of biomass) like glucose, fructose and cellulose.<sup>35, 36</sup> A series of intermediates and final products with extended carbon chains can be obtained through aldol condensation of FF and acetone followed by hydrogenation steps

(Scheme 1). Selective hydrogenation of monomer and dimer aldol products (scheme 1) produces increasingly saturated hydrogenated products (HPs) 1-9, and deeper hydrogenation of the HPs produces corresponding saturated alcohols or even alkanes (DHPs).<sup>2, 37</sup> In particular, the intermediates 3 and 8 are of great importance as they offer various options for further derivatization owing to the remaining carbonyl functional group. However, the carbonyl groups tend to be hydrogenated to alcohols (5 and 9) depending on factors such as solvent, partial pressure of hydrogen, and the nature of the catalyst. Hence a bifunctional catalyst that is catalytically active in the tandem two steps while still maintaining the final products to 3 and 8 with high selectivity is desirable.

Herein, we developed a bifunctional catalyst Pd/CN@MgO, where the support was composed of uniformly hybridized CN (nitrogen-containing carbon) and MgO, and the deposited Pd was finely dispersed. Application of this catalyst in the tandem aldol condensation-hydrogenation of furfural with acetone demonstrated excellent catalytic activity and high selectivity to the final hydrogenation products 3 and 8. Notably, DHPs were not produced in the present study.



**Scheme 1** Reaction network for tandem reactions of aldol condensation and the following possible reaction paths of hydrogenation steps.

## 25 Experimental

### Materials

PdCl<sub>2</sub> (59-60 wt%), D(+)-Glucosamine hydrochloride (99%), Magnesium oxide (50nm, spherical, 99.9% metals basis), furfural (AR, 99%) were used as received from Aladdin Chemistry Co., Ltd. NaBH<sub>4</sub> (96%), acetone (AR) were used as received from Sinopharm Chemical Reagent Co., Ltd. All solvents and chemicals were used without further treatment.

### Synthesis method

In a typical synthesis of 5% Pd/CN@MgO catalyst, firstly, 2.0 g GAH and 0.5 g MgO nanoparticles were thoroughly mixed together in a crucible with heating at 80 °C under stirring to evaporate the added water. It was then calcined at programmed temperature in a N<sub>2</sub> flow (400 mL/min) to 1000 °C for 1 h, until it was cooled down to room temperature. Black powder CN@MgO as catalyst support was obtained, then, 0.2 g CN@MgO and 2 mL 0.01 g/mL PdCl<sub>2</sub> solution were mixed well in 20 mL deionized water under ultrasound treatment. Afterwards, 10 mL of newly prepared NaBH<sub>4</sub> solution (1 mg/mL) was added to the above solution to obtain a ~ 5% Pd loading.

Later, the resultant product was filtered and washed with deionized water several times, after a drying process, the desired Pd/CN@MgO catalyst was ready to be used. In addition, Pd/CN, Pd/MgO and Pd/(MgO+CN) catalysts as comparisons were synthesized likewise except for a change of the catalyst supports.

### 50 Catalytic reactions

In a typical tandem aldol condensation-hydrogenation reaction of furfural with acetone, 40 mL H<sub>2</sub>O with thoroughly mixed 20 mg Pd/CN@MgO, 0.31g furfural and 1.69 g acetone were added into a 150 mL stainless-steel autoclave. The mixture was stirred for 1 h at 120 °C under 0.1 MPa N<sub>2</sub> as an aldol condensation step, followed by a hydrogenation step, under stirring, for 3 h at 120 °C with 1.0 MPa H<sub>2</sub>. When the above reaction was over and cooled down, the remaining H<sub>2</sub> was treated with a careful venting process, then the reaction mixture was extracted with ethyl acetate (~40 mL). The product distribution was analyzed by GC.

### Analytic methods and characterizations

The BET specific area was measured on a surface area and porosity analyzer (Micromeritics, ASAP 2020 HD88). Transmission electron microscopy (TEM) was carried out with a Hitachi HT-7700 microscope at an acceleration voltage of 100 kV. High-Resolution TEM (HRTEM), STEM-HAADF and STEM-EDX were performed on a Tecnai G2 F30 S-Twin at an acceleration voltage of 300 kV. X-Ray powder diffraction (XRD) patterns were measured on a Bruker D8 diffractometer equipped with a scintillation counter. Elemental analysis was obtained on a Vario El elemental analyser. The Pd dispersion was measured on a CHEMBET-3000 apparatus (Quantachrome Co.). Temperature programmed desorption of CO<sub>2</sub> (CO<sub>2</sub>-TPD) was performed on a TPD apparatus equipped with a thermal conductivity detector (TCD). The Pd contents were measured by inductively coupled plasma (ICP) Analysis and Nitric acid (70 wt%, semiconductor grade) was used to dissolve the sample. The FT-IR spectrum was collected on a Nicolet Nexus 470. All GC experiments were carried out and recorded by GC-MS (Agilent Technologies, GC 6890N, MS 5970). Thermogravimetric analysis (TGA) was conducted on a Thermogravimetric Analyzer (TGA 7, PERKIN ELMER). Raman spectra was measured on a raman spectrometer (JY, HR-800) using 514 nm laser. Optical contact angle with water was obtained on an interface tension meter (Kino SL 200KB).

## Results and discussion

In the present study, a bifunctional catalyst Pd/CN@MgO was obtained through a simple ultrasound-assisted reduction technique.<sup>38</sup> The CN@MgO hybrid with N-containing carbon and MgO were prepared through a drying procedure of the mixture of glucosamine hydrochloride (GAH) and MgO, followed by a thermal condensation process. As expected, the as-obtained Pd/CN@MgO exhibited the basicity of MgO, uniform small Pd size (2.2 nm in average size) with fine dispersion, excellent water dispersion and reaction stability. This indeed did a great favor on the reaction activity in our present study towards a tandem reaction that combines aldol condensation and selective hydrogenation of a bioderived compound.

Elemental analysis of the resulting CN@MgO hybrid had a

N/C atom ratio of 0.041 in the carbonaceous part (Table S1), which is an identification for successfully doping nitrogen into carbon (4.56% of nitrogen in mass proportion). Thermogravimetric analysis (TGA) of CN@MgO in O<sub>2</sub> flow revealed that the mass ratio of MgO in CN@MgO is ~ 40.0 % (Figure S2). The Raman spectrum (Fig. 1A) shows the characteristic D and G bands of amorphous carbon or disordered graphite of the prepared CN@MgO and CN with a similar I<sub>D</sub>/I<sub>G</sub> (I<sub>D</sub> represents the intensity of the D band, and I<sub>G</sub> represents the intensity of the G band) ratio of ~ 1.0. This indicates the carbonaceous part of CN@MgO maintains a very similar graphitic structure to that of N-containing carbon.<sup>10</sup> X-Ray diffraction (XRD) (Fig. 1B) of Pd/CN@MgO shows a relatively weak diffraction peak at ~ 26° which corresponds to graphitic carbon, and the diffraction peaks of Pd (111) and Pd (200) at ~ 40° and ~ 46° were observed. Strong and sharp peaks of MgO were also observed. Exact diffraction datas of MgO are in good agreement with MgO crystal (PDF#65-0476).

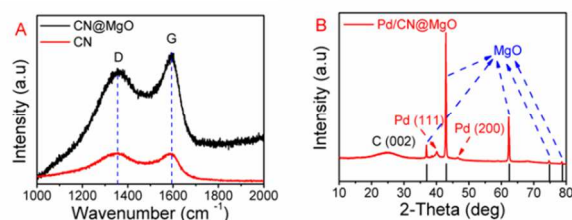


Fig. 1(A) Raman spectrum of CN@MgO and CN; (B) XRD patterns of the synthesized Pd/CN@MgO catalyst.

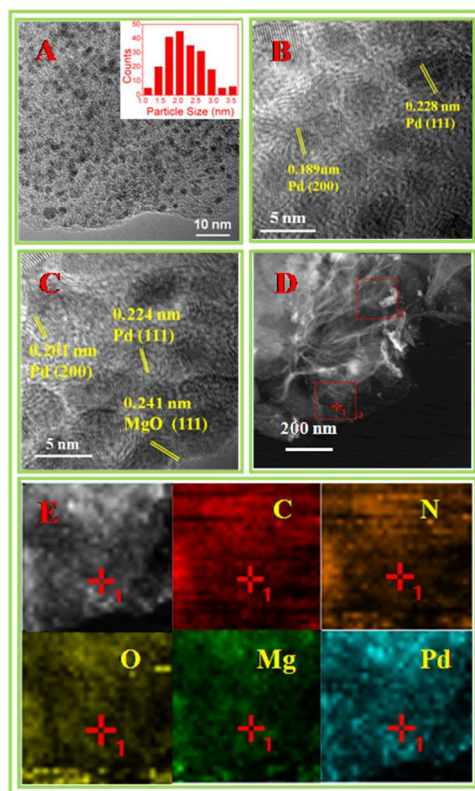


Fig. 2(A) HRTEM image showing uniform distribution of Pd NPs with particle size distribution of Pd NPs for ~ 200 particles of Pd/CN@MgO nanocomposite (in the inset); (B) HRTEM image displaying the crystal planes of the surface Pd NPs; (C) HRTEM image clearly showing the

amorphous morphology of carbon coating with uniform distribution of Pd nanoparticles (NPs); (D) A STEM HAADF image and (E) EDS maps of carbon, nitrogen, oxygen, magnesium and palladium of Pd/CN@MgO.

The high-resolution transmission electron microscopy (HRTEM) images of the synthesized Pd/CN@MgO catalyst are shown in Fig. 2. As for the difficulty in synthesizing supported Pd NPs with small size and uniform dispersion, and often capping or stabilizing agents were used<sup>39, 40</sup> which affects catalytic activity and perplexes preparation process, easy methods of synthesizing clean, small and uniformly dispersed supported Pd NPs are desirable. Attractively, through the simple ultrasound-assisted reduction technique which deposited Pd on the CN@MgO support, a uniform dispersion of Pd NPs (Figures 2A, S3) with an average particle size of 2.2 nm (inset in Fig. 2A) was observed. Inspired by the small Pd NPs with narrow distribution, the dispersion (*D*), i.e., the fraction of exposed Pd in the catalyst was further determined by CO chemisorption. Results showed that the *D* value for Pd/CN@MgO was determined to be 34%, suggesting a large number of active Pd atoms for H<sub>2</sub> chemisorption and activation, thus a high catalytic activity for hydrogenation can be expected. The HRTEM image in Fig. 2B revealed two kinds of crystal planes of Pd, and the crystal plane spacings were measured to be 0.224 and 0.198 nm. As to the structure of the hybrid support composed of MgO and N-doped carbon, we concluded that MgO was hybridized with carbon uniformly, as only local exposed MgO crystal lattice on the edge was observed in the HRTEM images of Pd/CN@MgO even at high magnifications (Fig. 2C). A STEM HAADF image and EDS were performed to verify the existence of MgO and nitrogen in the nanocomposites (Fig. 2D, 2E). Therefore, the HRTEM, Raman, and XRD investigations indicate that the Pd/CN@MgO hybrid material is composed of basic MgO uniformly hybridized with N-containing carbon, showing perfectly dispersed Pd NPs. Thus we may envision that it may possess some different catalytic properties.

Table 1 Aldol condensation of furfural with acetone with different catalyst support.

Entry	Cat.	Conv. (%)	Sel. (%)		
			Monomer	Dimer	Others
1	CN	0	0	0	0
2	MgO	87	86	14	0
3	CN+MgO	89	84	15	1
4	CN@MgO	>99	87	12	1

Reactions were carried under 0.1 MPa N<sub>2</sub> at 80 °C for 3h; All runs were carried out in 40 mL H<sub>2</sub>O with c(furfural)=0.081 mol·L<sup>-1</sup> while keeping the molar ratio of furfural/acetone 1:9 and the mass ratio of organic/catalyst 100:1.

For comparisons, a series of supports CN, MgO, and CN+MgO were prepared to compare their aldol condensation ability with CN@MgO. As seen in Table 1, CN alone showed no aldol catalytic ability due primarily to its weak basicity. Interestingly, CN@MgO displayed the best catalytic activity towards aldol condensation at 80 °C for 3 h under N<sub>2</sub> atmosphere, achieving ~ 99% furfural conversion. The better condensation activity of the CN@MgO was due to the following factors: 1) The basicity was maintained because of the component MgO in the CN@MgO; 2) The good dispersion of the hybrid in the reaction solutions by introducing of hydrophilic N-containing carbon<sup>10</sup>(Figure S4A); 3)

The lower specific gravity of carbon materials than MgO that again enables the hybrid to better disperse in water (Figure S4B); 4) The porous structure of the carbon surrounding the MgO matrix (Table S2). Furthermore, CO<sub>2</sub>-TPD investigations of the catalyst supports proved that the MgO in the CN@MgO hybrid may have endowed the surrounded CN with new active sites for aldol condensation (Figure S5). The above outstanding features of the hybrid catalyst thus improved the exposure of the active sites toward the substrates (like furfural and acetone) and finally enhanced the catalytic performance significantly. Then Pd NPs were further deposited on CN@MgO to form a bifunctional catalyst Pd/CN@MgO, in order to investigate its enhanced catalytic activity that combines both aldol condensation and hydrogenation in a one-pot reactor to simplify reaction steps. Also, for comparisons, a series of catalysts Pd/MgO, Pd/CN, Pd/(MgO+CN) were all synthesized through the simple ultrasound-assisted reduction technique. Theoretically, all of the synthesized Pd catalysts were done with 5.66 wt% Pd in mass ratio, and actual Pd loading by ICP analysis was 4.6%, 6.0%, 5.4% and 5.6% for Pd/CN, Pd/MgO, Pd/(MgO+CN) and Pd/CN@MgO, respectively.

**Table 2** Catalytic products of tandem aldol condensation-hydrogenation of furfural with acetone by Pd supported catalysts.

Entry	Cat. <sup>a</sup>	Conv. <sup>b</sup> (%)	Sel. <sup>c</sup> (%)			
			1	3	7	8
1	Pd/CN	0	0	0	0	0
2 <sup>d</sup>	Pd/MgO	86	39	42	5	6
3	Pd/(CN+MgO)	74	12	77	0	11
4	Pd/CN@MgO	>99	0	82(2)	0	14(2)

<sup>a</sup> Theoretically synthesized with 5.66 wt% Pd in mass ratio. <sup>b</sup> Furfural conversion in the aldol condensation. <sup>c</sup> Products distribution in the hydrogenation process. <sup>d</sup> Other 8 % products were detected. All runs were carried out in 40 mL H<sub>2</sub>O with c (furfural) = 0.081 mol·L<sup>-1</sup> while keeping the molar ratio of furfural/acetone 1:9 and the mass ratio of organic/catalyst 100:1. Condensation in 0.1 MPa N<sub>2</sub>, 80 °C for 3 h; Hydrogenation in 1.7 MPa H<sub>2</sub>, 120 °C for 3 h. Where the brackets are the corresponding alcohols.

Table 2 gives an overview of the catalytic systems of our study. Unsurprisingly, Pd/CN@MgO showed the best catalytic activity towards the aldol reaction with ~ 99% furfural conversion, much higher than that of both Pd/MgO and Pd/(MgO+CN), demonstrating that after the addition of Pd NPs the catalytic condensation activity was unaffected. In addition, Pd/MgO and Pd/(MgO+CN) catalysts displayed relatively broad product mixtures while Pd/CN@MgO exhibited a better selectivity towards the products 3 and 8. This indicates that variation of the catalyst support can control selectivity. That is to say, the simple physical mixture of CN and MgO was incapable of achieving a higher catalytic activity than Pd/CN@MgO which was more favorable for the aldol reaction. As observed from TEM images in Figures 2A and S3, Pd/CN@MgO showed small Pd size with a narrow size distribution, totally unlike the obvious Pd NPs aggregation of Pd/(CN+MgO) (Figure S6), and much smaller than the Pd size (~ 4.9 nm) on previously reported Pd@CN<sub>0.132</sub> catalyst with N-doped carbon alone as a support (Figure S7).<sup>10</sup> This demonstrates the synergic effect of the two components of the CN@MgO hybrid towards the anchored Pd NPs. What's more, the hydrophilic property of the Pd/CN@MgO in the reaction media, again, strengthened its exposure to the

substrates, so increased catalytic performance was obtained. Still, BET specific area of Pd/MgO, Pd/(CN+MgO) and Pd/CN@MgO were 44, 106 and 172 m<sup>2</sup>g<sup>-1</sup>, respectively (Table 3 for textural analysis and figure S8 for adsorption/desorption isotherms), which was also in accordance with the total catalytic activity. Therefore, these results strongly suggest that the Pd/CN@MgO nanocomposite would be used as the desired bifunctional catalyst to further optimize its reaction conditions to maximize our desired products 3 and 8.

**Table 3** BET specific area, pore volume and average pore size of the catalysts determined by nitrogen sorption measurements.

Entry	Catalyst	S <sub>BET</sub> (m <sup>2</sup> g <sup>-1</sup> )	Pore volume (cm <sup>3</sup> /g)	Average pore size (nm)
1	Pd/MgO	44	0.22	20
2	Pd/(CN+MgO)	106	0.28	10
3	Pd/CN@MgO	172	0.29	7

To get a better understanding of the process of gradual hydrogenation of aldol products by Pd/CN@MgO, the monomer was chosen as the substrate to conduct the monitoring by sampling at 60 °C under 0.1 MPa H<sub>2</sub> for a detailed investigation (Fig. 3). At first both the C=C double bond and the heteroaromatic ring of the monomer were hydrogenated but with a faster rate for C=C double bond, followed by total hydrogenation of the heteroaromatic ring to transform the unsaturated products to saturated product 3, with negligible C=O double bond being hydrogenated (See figure S9 for detailed products identification by GC-MS). The selectivity of Pd/CN@MgO in the hydrogenation of the various functional groups allows to selectively obtain 3 and 8 as the main products of the reaction in the present study.

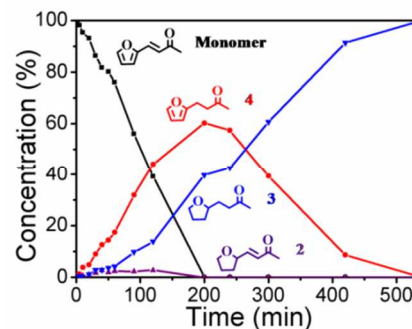


**Fig. 3** Evolution of reactant and product selectivity as a function of time using Pd/CN@MgO as a catalyst under 0.1 MPa H<sub>2</sub> at 60 °C.

The monitoring of the hydrogenation process of the monomer gave access to a better understanding of the intermediates and final products in the consecutive reactions. As the present catalytic process includes aldol condensation and hydrogenation steps for the synthesized bifunctional catalyst Pd/CN@MgO, so optimized aldol condensation conditions are required to achieve a desired conversion of furfural. Thus, we first studied different reaction parameters for aldol condensation between furfural and acetone using Pd/CN@MgO. Therefore, N<sub>2</sub> pressure, molar ratio of the substrates, reaction time and temperature were chosen as the parameters (Table S3). When considering both conversion and monomer selectivity, a molar ratio of furfural to acetone of 1:9 with excess acetone at 80 °C for 3 h under 0.1 MPa N<sub>2</sub> was able to achieve > 99% furfural conversion (entry 2). When the

reaction was conducted at 120 °C in 0.1 MPa N<sub>2</sub>, 1 h was enough for > 99% furfural conversion while still retaining monomer selectivity (entry 8), but ~ 95% conversion was obtained for further shortened reaction time of 0.5 h (entry 9), so condensation at 120 °C for 1 h in 0.1 MPa N<sub>2</sub> with furfural/acetone being 1:9 was used for sequential hydrogenation investigation in the following studies.

**Table 4** Effects of different parameters for hydrogenation of the aldol condensation products using Pd/CN@MgO.

Entry	H <sub>2</sub> (MPa)	Temp. (°C)	Time (h)	Sel. <sup>a</sup> (%)			
				1	3	8	Others
1	0.5	120	3	7	76(1)	12(0)	4
2	1.0	120	3	0	84(1)	11(1)	3
3	1.0	100	5	1	82(1)	13(1)	2
4	2.0	100	5	0	82(2)	13(1)	2
5	3.0	100	3	1	80(3)	13(2)	1
6	3.0	200	15	0	19(67)	1(11)	2

<sup>a</sup>Conversion of the hydrogenation process was 100% for all the reactions. The brackets are the corresponding alcohols. All runs were carried out in 40 mL H<sub>2</sub>O with c (furfural) = 0.081 mol·L<sup>-1</sup> while keeping the molar ratio of furfural/acetone 1:9 and the mass ratio of organic/catalyst 100:1, and the hydrogenation reactions were all following the first step of aldol condensation between furfural and acetone in 0.1 MPa N<sub>2</sub>, 120 °C for 1 h as a sequential reaction system.

Having performed the excellent aldol condensation ability of the Pd/CN@MgO catalyst, a following hydrogenation step was investigated that well represented its bifunctionality for facilitating a single-reactor, aqueous process that combines aldol condensation with sequential hydrogenation. Hydrogenation of the aldol products (monomer and dimer) results in a series of HPs and DHPs (Scheme 1). Focusing on getting the intermediate 3 and 8 with high selectivity as possible, the hydrogenation conditions of hydrogen pressure, reaction temperature and time were selected for further optimization (Table 4). Obviously, high targets (3 and 8) selectivity of 95% can be achieved at 120 °C under 1.0 MPa H<sub>2</sub> (entry 2), and lower H<sub>2</sub> pressure of 0.5 MPa was not capable for total conversion to our targets (entry 1). Then, when the temperature was decreased to 100 °C under 1.0 MPa H<sub>2</sub>, a longer time of 5 h was needed for an equal selectivity (entry 3). And results showed that even at 3.0 MPa H<sub>2</sub> for 3h, there was still hydrogenation product 1 (1%) that was not hydrogenated to 3 together with excessive hydrogenated products of our targets (entry 5). However, when the catalytic hydrogenation was performed at reaction conditions of 200 °C under 3.0 MPa H<sub>2</sub> for 15 h, 78 % selectivity for alcohols (5 and 9) was obtained (entry 6).

**Table 5** Results of catalyst recycles towards hydrogenation of monomer using Pd/CN@MgO.

Entry	Recycle runs	Conv. (%)	Sel. (%)		
			3	1	5
1	Fresh	100	98	0	2
2	1 <sup>st</sup>	100	98	1	1
3	2 <sup>nd</sup>	100	93	5	2
4	3 <sup>rd</sup>	100	97	2	1

Reaction conditions: monomer 0.1 g, catalyst 40 mg, water 20 mL, H<sub>2</sub> pressure 0.1 MPa, 80 °C, 1.5 h. For each of the recycles, the amount of substrate was reduced in proportion with the recycled catalyst.

Furthermore, ICP measurement was performed to investigate the Pd loss of Pd/CN@MgO in the above reaction conditions, and no Pd was detected, suggesting negligible Pd was lost in the tandem reaction process. Recycling experiments of the hydrogenation process proved that the catalyst is highly stable and can be reused several times without the loss of its catalytic activity (Table 5). The above results demonstrated the deposited Pd NPs were finely anchored on the support, and the reason was due much to the doped nitrogen of the carbon structure in retaining metal NPs.<sup>10</sup> As is known, MgO is easily hydrolyzed to Mg(OH)<sub>2</sub> during hydrothermal treatment, which makes it unstable during reactions in aqueous media. However, in the present study, Pd/CN@MgO demonstrated its excellent support stability in the above tandem reaction conditions in water, showing negligible transformation of MgO into Mg(OH)<sub>2</sub> (Figure S10A). That is a strong evidence that the carbon structure can also help in stabilizing MgO, which also proves that MgO was hybridized with carbon uniformly (Figure 2C). However, without protection and stabilization of the carbon coating, the Pd/MgO catalyst is completely hydrolysed (Figure S10B), again illustrating the important function of the carbon structure in the stabilization of catalyst supports.

## Conclusions

In summary, a bifunctional Pd/CN@MgO catalyst was prepared by a very simple ultrasound-assisted reduction technique which can deposit Pd NPs on a bioderived nitrogen-doped carbon coated MgO (CN@MgO) hybrid and this catalyst has uniform small Pd NPs with 2.2 nm in average size and fine dispersion. Since the introduction of the hydrophilic N-containing carbon structure to MgO by thermal condensation, this catalyst also shows both nice water dispersion and reaction stability. With such improved features, this catalyst showed a high catalytic ability in a tandem aldol condensation-hydrogenation reaction of furfural with acetone in a single reactor, obtaining > 99% furfural conversion and 95% hydrogenation products selectivity (84% of 3 and 11% of 8). This bifunctional catalyst opens up a new access for upgrading biomass-derived intermediates and the catalyst designing strategy provides new ways for construction of metal supported bi/multi-functional catalysts with good particle distribution along with improved catalyst hydrophilic property. Further work will be oriented to expending other metal(s) and support structure modification, with expectations for wider application in other model systems.

## Acknowledgements

Financial support from the National Natural Science Foundation of China (21376208&U1162124), the Zhejiang Provincial Natural Science Foundation for Distinguished Young Scholars of China (LR13B030001), the Specialized Research Fund for the Doctoral Program of Higher Education (J20130060), the Fundamental Research Funds for the Central Universities, the Program for Zhejiang Leading Team of S&T Innovation, the Partner Group Program of the Zhejiang University and the Max-Planck Society are greatly appreciated.

## Notes and references

Carbon Nano Materials Group, ZJU-NHU United R&D Center, Department of Chemistry, Zhejiang University, Hangzhou 310028, P. R. China.

Email: chemwy@zju.edu.cn. Fax: (+86)-571-8795-1895.

† Electronic Supplementary Information (ESI) available: Detailed experimental procedures, Figures S1-S10 and Tables S1-S4. See DOI: 10.1039/b000000x/

1. I. Fechete, Y. Wang and J. C. Védrine, presented in part at the Catal. Today, 2012.
2. G. W. Huber, J. N. Chheda, C. J. Barrett and J. A. Dumesic, *Science*, 2005, **308**, 1446-1450.
3. X. Huang, C. Guo, J. Zuo, N. Zheng and G. D. Stucky, *Small*, 2009, **5**, 361-365.
4. K. Yoon, Y. Yang, P. Lu, D. Wan, H. C. Peng, K. Stamm Masias, P. T. Fanson, C. T. Campbell and Y. Xia, *Angew. Chem. Int. Ed.*, 2012, **51**, 9543-9546.
5. S. H. Joo, J. Y. Park, C.-K. Tsung, Y. Yamada, P. Yang and G. A. Somorjai, *Nat. Mater.*, 2009, **8**, 126-131.
6. H. Liu, T. Jiang, B. Han, S. Liang and Y. Zhou, *Science*, 2009, **326**, 1250-1252.
7. X. Gu, Z.-H. Lu, H.-L. Jiang, T. Akita and Q. Xu, *J. Am. Chem. Soc.*, 2011, **133**, 11822-11825.
8. M. Meilikhov, K. Yusenko, D. Esken, S. Turner, G. Van Tendeloo and R. A. Fischer, *Eur. J. Inorg. Chem.*, 2010, **2010**, 3701-3714.
9. A. La Torre, M. d. C. Giménez-López, M. W. Fay, G. A. Rance, W. A. Solomonsz, T. W. Chamberlain, P. D. Brown and A. N. Khlobystov, *ACS Nano*, 2012, **6**, 2000-2007.
10. X. Xu, Y. Li, Y. Gong, P. Zhang, H. Li and Y. Wang, *J. Am. Chem. Soc.*, 2012, **134**, 16987-16990.
11. D. J. Davis, A.-R. O. Raji, T. N. Lambert, J. A. Vigil, L. Li, K. Nan and J. M. Tour, *Electroanalysis*, 2014, **26**, 164-170.
12. X. Pan, Z. Fan, W. Chen, Y. Ding, H. Luo and X. Bao, *Nat. Mater.*, 2007, **6**, 507-511.
13. J. Kang, S. Zhang, Q. Zhang and Y. Wang, *Angew. Chem. Int. Ed.*, 2009, **48**, 2565-2568.
14. P. Zhang, J. Yuan, T. P. Fellingner, M. Antonietti, H. Li and Y. Wang, *Angew. Chem. Int. Ed.*, 2013, **52**, 6028-6032.
15. W. Lin, H. Cheng, J. Ming, Y. Yu and F. Zhao, *J. Catal.*, 2012, **291**, 149-154.
16. S. Crossley, J. Faria, M. Shen and D. E. Resasco, *Science*, 2010, **327**, 68-72.
17. M. P. Ruiz, J. Faria, M. Shen, S. Drexler, T. Prasomsri and D. E. Resasco, *ChemSusChem*, 2011, **4**, 964-974.
18. C. J. Barrett, J. N. Chheda, G. W. Huber and J. A. Dumesic, *Appl. Catal., B*, 2006, **66**, 111-118.
19. J. Julis and W. Leitner, *Angew. Chem. Int. Ed.*, 2012, **51**, 8615-8619.
20. A. Corma, T. Rodenas and M. J. Sabater, *Chem. Eur. J.*, 2010, **16**, 254-260.
21. B. Peng, Y. Yao, C. Zhao and J. A. Lercher, *Angew. Chem. Int. Ed.*, 2012, **51**, 2072-2075.
22. A.-H. Lu, G.-P. Hao, Q. Sun, X.-Q. Zhang and W.-C. Li, *Macromol. Chem. Phys.*, 2012, **213**, 1107-1131.
23. Y. Zhai, Y. Dou, D. Zhao, P. F. Fulvio, R. T. Mayes and S. Dai, *Adv. Mater.*, 2011, **23**, 4828-4850.
24. B. Hu, K. Wang, L. Wu, S. H. Yu, M. Antonietti and M. M. Titirici, *Adv. Mater.*, 2010, **22**, 813-828.
25. L. Zhao, N. Baccile, S. Gross, Y. Zhang, W. Wei, Y. Sun, M. Antonietti and M.-M. Titirici, *Carbon*, 2010, **48**, 3778-3787.
26. S. Maldonado and K. J. Stevenson, *J. Phys. Chem. B*, 2005, **109**, 4707-4716.
27. L. Zhao, L. Z. Fan, M. Q. Zhou, H. Guan, S. Qiao, M. Antonietti and M. M. Titirici, *Adv. Mater.*, 2010, **22**, 5202-5206.
28. Y.-H. Li, T.-H. Hung and C.-W. Chen, *Carbon*, 2009, **47**, 850-855.
29. G.-X. Chen, J.-M. Zhang, D.-D. Wang and K.-W. Xu, *Physica B*, 2009, **404**, 4173-4177.
30. Z. Li, J. Liu, C. Xia and F. Li, *ACS Catal.*, 2013, **3**, 2440-2448.
31. Y. Wang, J. Yao, H. Li, D. Su and M. Antonietti, *J. Am. Chem. Soc.*, 2011, **133**, 2362-2365.
32. Y. Gong, P. Zhang, X. Xu, Y. Li, H. Li and Y. Wang, *J. Catal.*, 2013, **297**, 272-280.
33. P. Zhang, Y. Gong, H. Li, Z. Chen and Y. Wang, *Nature communications*, 2013, **4**, 1593.
34. A. M. Frey, J. Yang, C. Feche, N. Essayem, D. R. Stellwagen, F. Figueras, K. P. de Jong and J. H. Bitter, *J. Catal.*, 2013, **305**, 1-6.
35. H. Zhao, J. E. Holladay, H. Brown and Z. C. Zhang, *Science*, 2007, **316**, 1597-1600.
36. E. I. Gurbuz, J. M. Gallo, D. M. Alonso, S. G. Wettstein, W. Y. Lim and J. A. Dumesic, *Angew. Chem. Int. Ed.*, 2013, **52**, 1270-1274.
37. A. D. Sutton, F. D. Waldie, R. Wu, M. Schlaf, Louis A. 'Pete' Silks III and J. C. Gordon, *Nat. Chem.*, 2013, **5**, 428-432.
38. Y. Li, X. Xu, P. Zhang, Y. Gong, H. Li and Y. Wang, *RSC Adv.*, 2013, **3**, 10973.
39. V. Mazumder and S. Sun, *J. Am. Chem. Soc.*, 2009, **131**, 4588-4589.
40. J. A. Lopez-Sanchez, N. Dimitratos, C. Hammond, G. L. Brett, L. Kesavan, S. White, P. Miedziak, R. Tiruvalam, R. L. Jenkins, A. F. Carley, D. Knight, C. J. Kiely and G. J. Hutchings, *Nat. Chem.*, 2011, **3**, 551-556.
41. N. Mahata and V. Vishwanathan, *J. Catal.*, 2000, **196**, 262-270.